



This is a repository copy of *Correlation between the secondary structure and surface activity of β -sheet forming cationic amphiphilic peptides and their anticancer activity.*

White Rose Research Online URL for this paper:

<https://eprints.whiterose.ac.uk/180079/>

Version: Accepted Version

Article:

Hadianamrei, R., Tomeh, M.A., Brown, S. orcid.org/0000-0002-7581-7491 et al. (2 more authors) (2021) Correlation between the secondary structure and surface activity of β -sheet forming cationic amphiphilic peptides and their anticancer activity. *Colloids and Surfaces B: Biointerfaces*, 209 (Part 2). 112165. ISSN 0927-7765

<https://doi.org/10.1016/j.colsurfb.2021.112165>

© 2021 Elsevier B.V. This is an author produced version of a paper subsequently published in *Colloids and Surfaces B: Biointerfaces*. Uploaded in accordance with the publisher's self-archiving policy. Article available under the terms of the CC-BY-NC-ND licence (<https://creativecommons.org/licenses/by-nc-nd/4.0/>).

Reuse

This article is distributed under the terms of the Creative Commons Attribution-NonCommercial-NoDerivs (CC BY-NC-ND) licence. This licence only allows you to download this work and share it with others as long as you credit the authors, but you can't change the article in any way or use it commercially. More information and the full terms of the licence here: <https://creativecommons.org/licenses/>

Takedown

If you consider content in White Rose Research Online to be in breach of UK law, please notify us by emailing eprints@whiterose.ac.uk including the URL of the record and the reason for the withdrawal request.



eprints@whiterose.ac.uk
<https://eprints.whiterose.ac.uk/>

Statistical summary

1
2
3
4
5
6
7

Total number of words: 9189

Total number of tables: 2

Total number of figures: 6

Correlation between the secondary structure and surface activity of β -sheet forming cationic amphiphilic peptides and their anticancer activity

Roja Hadianamrei¹, Mhd Anas Tomeh¹, Stephen Brown³, Jiqian Wang⁴, Xiubo Zhao^{1,2*}

¹ Department of Chemical and Biological Engineering, University of Sheffield, S1 3JD, UK.

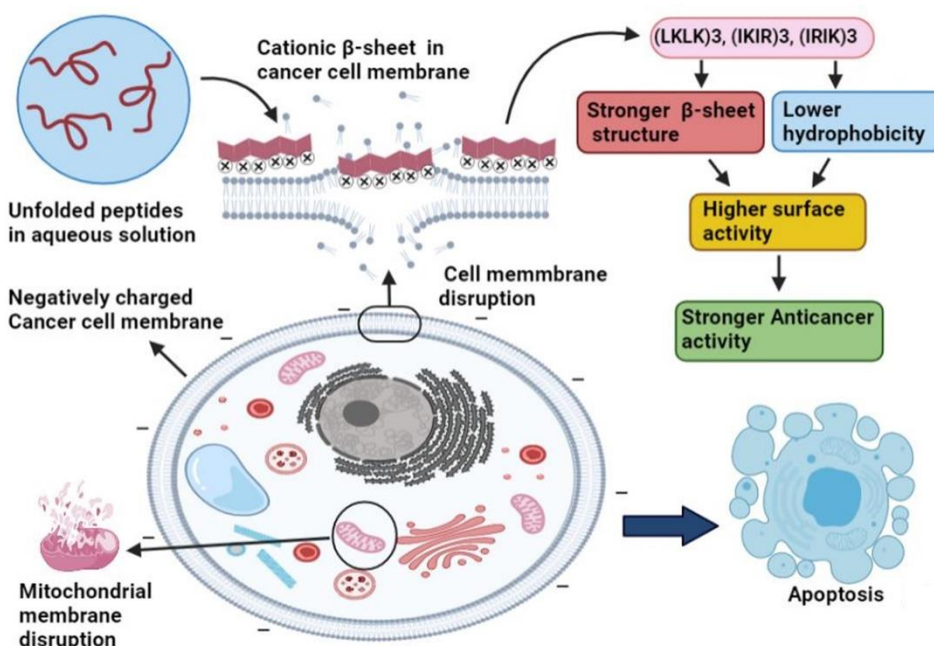
² School of Pharmacy, Changzhou University, Changzhou 213164, China.

³ Department of Biomedical Science, University of Sheffield, S10 2TN, UK.

⁴ Centre for Bioengineering and Biotechnology, China University of Petroleum (East China), Qingdao 266555, China.

*Corresponding author: E-mail: xiubo.zhao@sheffield.ac.uk Tel: +44-(0)-114-222-8256

Graphral Abstract



23

24 Abstract

25 Cancer is one of the main causes of death worldwide. The current cancer treatment strategies
26 often lack selectivity for cancer cells resulting in dose-limiting adverse effects and reduced quality of
27 life. Recently, anticancer peptides (ACPs) have emerged as an alternative treatment with higher
28 selectivity, less adverse effects, and lower propensity for drug resistance. However, most of the
29 current studies on the ACPs is focused on α -helical ACPs and there is lack of systematic studies on
30 β -sheet forming ACPs. Herein we report the development of a new series of rationally designed short
31 cationic amphiphilic β -sheet forming ACPs and their structure activity relationship. The peptides had
32 the general formula $(XY_1XY_2)_3$, with X representing hydrophobic amino acids (isoleucine (I) or leucine
33 (L)), Y_1 and Y_2 representing cationic amino acids (arginine (R) or lysine (K)). The cytotoxicity of the
34 designed ACPs in HCT 116 colorectal cancer, HeLa cervical cancer and human dermal fibroblast
35 cells was assessed by MTT test. The physicochemical properties of the peptides were characterized
36 by various techniques including RP-HPLC, LC-MS, and Circular Dichroism (CD) spectroscopy. The
37 surface activity of the peptides at the air-water interface and their interaction with the lipid monolayers
38 as models for cell membranes were studied by Langmuir trough. The peptides consisting of I with R
39 and K had selective anticancer activity while the combination of L and R diminished the anticancer
40 activity of the peptides but rendered them more toxic to HDFs. The anticancer activity of the peptides
41 was directed by their surface activity (amphiphilicity) and their secondary structure in hydrophobic
42 surfaces including cancer cell membranes. The selectivity of the peptides for cancer cells was a
43 result of their higher penetration into cancer cell membranes compared to normal cell membranes.
44 The peptides exerted their anticancer activity by disrupting the mitochondrial membranes and
45 eventually apoptosis. The results presented in this study provide an insight into the structure-activity
46 relationship of this class of ACPs which can be employed as guidance to design new ACPs with
47 improved anticancer activity and lower toxicity against normal cells.

48

49 *Keywords: Anticancer peptides; cationic amphiphilic peptides; beta sheet peptides; cervical cancer;*
50 *colorectal cancer; surface activity.*

51

52

53 1. Introduction

54 Cancer is caused by genetic mutations in the “driver genes” which renders the cancer cells
55 capable of evading growth suppression, resisting cell death, and metastasizing¹⁻⁴. It has become a
56 major global health concern and one of the main causes of death worldwide. The currently available
57 antineoplastic agents often lack selectivity for cancer cells and cause damage to healthy tissues
58 leading to adverse effects that could be dose-limiting or reduce the patient’s quality of life⁵⁻¹³. The
59 development of multidrug resistance (MDR) is another major concern associated with conventional
60 anticancer drugs^{5, 14}. Although immunotherapy with monoclonal antibodies, immune checkpoint
61 inhibitors and modified immune cells^{3, 15-24} more selectively targets the cancer cells, it is still
62 associated with dose-limiting adverse effects and in some cases lethal hypersensitivity reactions²⁴⁻
63²⁹. Furthermore, the complexity and high costs of manufacturing place immunotherapy drugs among
64 the most expensive drugs in the market^{24, 27, 30, 31}. Hence, there is still a quest for the development
65 of new anticancer drugs with high selectivity for cancer cells, low propensity for drug resistance and
66 low production costs.

67 Recently, anticancer peptides (ACPs) have been introduced as an alternative to conventional
68 antineoplastic agents. Naturally occurring host defence peptides with antimicrobial or antifungal
69 activity are found in different organisms including plants, insects, amphibians, and mammals³²⁻³⁶.
70 Some of these peptides also possess selective anticancer activity³⁵⁻³⁷. Due to their smaller size and
71 higher solubility compared to monoclonal antibodies and checkpoint inhibitors, the ACPs enjoy better
72 pharmacokinetics and higher cellular uptake which could enhance their potency and efficacy³⁸.

73 It is well evidenced that the higher selectivity of the ACPs for cancer cells compared to normal
74 cells lies in the higher affinity of these cationic peptides for the anionic membrane of the cancer cells
75 compared to the zwitterionic membrane of the normal cells^{32-37, 39}. The more negative charge of the
76 cancer cell membranes is due to the presence of negatively charged phospholipids
77 phosphatidylserine (PS) and higher abundance of anionic molecules such as heparan sulfates and
78 O-glycosylated mucins^{32-37, 39}. Since the ACPs target the cancer cell membranes, their selectivity for
79 cancer cells is less affected by the tumour heterogeneity and also, they are less prone to drug
80 resistance which is one of their advantages over the other types of anticancer agents^{33, 35, 36}. Over
81 the last decade, more research has been directed towards developing synthetic ACPs to reduce
82 their production costs, improve their physicochemical properties, enhance their resistance to
83 enzymatic proteolysis, and reduce their risk of immunogenicity^{35, 40-48}. Despite the large amount of
84 literature on the structure activity relationship (SAR) of the α -helical antimicrobial and anticancer
85 peptides, there are very few studies on β -sheet forming peptides and most of these studies have
86 focused on the antimicrobial activity⁴⁹⁻⁵³ and there are very few studies on SAR of β -sheet forming
87 anticancer peptides^{52, 54}. Hence, there is the need for systematic studies correlating the structure
88 and physicochemical properties of the β -sheet forming peptides to their potential anticancer activity
89 and selectivity.

90 Herein we report the development of a new series of de novo designed β -sheet forming anticancer
91 peptides with selective anticancer activity against colorectal and cervical cancer cells. The
92 cytotoxicity of the designed peptides in cancer cells and normal cells was assessed with regard to
93 their physicochemical properties. Furthermore, the tendency of the peptides to penetrate into
94 different types of lipid mono and bilayers mimicking normal and cancer cell membranes were studied
95 to provide an insight into the mechanism of cell selectivity of these peptides. The general formula for
96 this series of peptides is $(XY_1XY_2)_3$, with X representing hydrophobic amino acids (isoleucine (I) or
97 leucine (L)), Y_1 and Y_2 representing cationic amino acids (arginine (R) or lysine (K)). The peptides
98 were designed using de novo minimalist design approach based on the common occurrence of
99 amphipathic dyad repeats in β -sheet forming peptides which allows for orientation of alternating
100 residues toward alternating faces of the β -sheet^{49, 51, 55}. The choice of the hydrophobic amino acids
101 was based on their high propensity for forming β -sheets and their high occurrence in β -sheets in
102 naturally occurring proteins⁵⁶⁻⁵⁹. The cationic (hydrophilic) amino acids were chosen based on their
103 high abundance in the naturally occurring β -sheet forming peptides⁵⁹. The peptides were amidated
104 at the C-terminal to enhance their anticancer activity by increasing the positive charge density⁶⁰⁻⁶².
105 The current study also uses a systematic approach by keeping the length and the net positive charge
106 of the peptides constant while changing the amino acid combination in the repeat unit to investigate
107 the effect of such structural changes on the β -sheet forming tendency, the anticancer activity, and
108 cell selectivity of the resulting peptides. Although this combination of hydrophobic and cationic amino
109 acids has been previously used for developing β -sheet forming antimicrobial peptides with different
110 sizes and sequences^{49, 51}, to the best of our knowledge there have been no reports on anticancer
111 peptides with these structures. Furthermore, while the structure-activity relationship of the α -helical
112 AMPs and ACPs have been widely studied, there is very limited literature data on the structure
113 activity relationship of the β -sheet forming AMPs and none on the β -sheet forming ACPs.

114 2. Materials and methods

115 Materials

116 The peptides were synthesized by Fmoc solid-phase synthesis using a commercial CEM Liberty
117 peptide synthesizer. The synthesis was carried out from the C-terminus to the N-terminus on the
118 Rink amide MBHA resin, thus producing C-terminally amidated peptides. The peptides were purified
119 by cold ether precipitation eight times to reach the purity of >95%, followed by lyophilization for 2
120 days. The peptide solutions were prepared by dissolving the lyophilized peptide powders in Milli-Q
121 water (Millipore Reagent Water System, USA) and their pH was adjusted to the desirable range
122 using sodium hydroxide. All the chemicals, reagents and organic solvents were sourced from Merck
123 (Sigma Aldrich), UK, with analytical grade. Rink amide-methylbenzhydrylamine hydrochloride salt
124 (MBHA) resin, and 9-fluorenyl-methoxycarbonyl (Fmoc) protected amino acids were bought from GL
125 Biochem Ltd (Shanghai, China). 1,2-dipalmitoyl-sn-glycero-3-phosphocholine (DPPC) and 1,2-
126 dipalmitoyl-sn-glycero-3-phospho-(1'-rac-glycerol) (DPPG) were purchased from Avanti Polar Lipids

127 (USA). The Dulbecco's Modified Eagle Medium (DMEM), Phosphate buffered saline (PBS), Fetal
128 bovine serum (FBS), Trypsin, Penicillin and streptomycin were sourced from GIBCO (Thermo Fisher
129 Scientific, UK). JC-1 mitochondrial probe (Invitrogen™) was sourced from Invitrogen (Thermo Fisher
130 Scientific, UK).

131 Determination of peptide sequence and purity

132 The peptide sequences and molecular weights were verified by Liquid chromatography-Mass
133 spectrometry (LC-MS) (QExactive HF, Thermo Fisher™). The full MS scan from m/z= 375-1500 was
134 acquired in the Orbitrap at a resolution of 120,000. Subsequent fragmentation was Top 2 in the HCD
135 cell, with detection of ions in the Orbitrap using centroid mode, with a resolution of 30,000. The purity
136 of the peptides was checked by reverse phase high performance liquid chromatography (RP-HPLC)
137 using Waters 2695 HPLC system, with Waters 2487 UV/Visible detector, and Xbridge C18 column
138 (4.6 x 250 mm). The mobile phase consisted of Acetonitrile and Trifluoroacetic acid (TFA) in water
139 (0.1% V/V), with a gradient of 5% to 95% Acetonitrile over 20 mins at a flow rate of 1 mL/min.

140 Determination of peptide hydrophobicity

141 The hydrophobicity of the designed peptides was determined both theoretically using the
142 Eisenberg method^{63, 64} and experimentally using RP-HPLC retention times. The mean
143 hydrophobicity value for each peptide was calculated using the following equation:

$$144 \quad \langle H \rangle = (\sum_{i=1}^N H_i) / N \quad \text{Eq. 1.}$$

145 Where $\langle H \rangle$ is the mean hydrophobicity of the peptide sequence, H_i is the hydrophobicity of each
146 amino acid in the peptide sequence and N is the number of amino acid residues^{63, 64}. The
147 hydrophobicity of amino acids was based on their octanol-water partition coefficients as reported by
148 Fauchère and Pliska^{65, 66}.

149 Determination of peptide secondary structure

150 The secondary structure of the peptides was determined by Circular Dichroism (CD) spectroscopy
151 using a Jasco J-810 spectropolarimeter and a quartz cell with 1 cm path length. The samples were
152 scanned in the far UV ($\lambda = 190-240$ nm), at a scanning speed of 100 nm/min and a fixed peptide
153 concentration (10 μ M). The CD measurements were performed on peptides in aqueous solution and
154 in three different types of curved lipid bilayers: Sodium dodecyl sulfate (SDS) micelles, DPPG small
155 unilamellar vesicles (SUVs) and DPPC SUVs. All measurements were performed in triplicate and
156 the data were reported as the average of the three repeats. The mean residue molar ellipticity was
157 calculated using the following equation:

$$158 \quad \theta_M = \frac{\theta_{obs}}{10} \cdot \frac{M_{RW}}{c \cdot l} \quad \text{Eq. 2.}$$

159 Where θ_M is residue molar ellipticity ($\text{deg.cm}^2.\text{dmol}^{-1}$), θ_{obs} is the observed ellipticity at a given
160 wavelength (mdeg), M_{RW} is residue molecular weight obtained by dividing the molecular weight of

161 the peptide by the number of amino acid residues, c is the peptide concentration (mg/mL), and l is
162 the path length of the cell (cm) ^{49, 50, 67-69}.

163 Preparation of lipid vesicles

164 The DPPC and DPPG SUVs were prepared by thin-film hydration method. Briefly, a thin lipid film
165 was produced from lipid solution in chloroform (at a concentration of 2 mg/mL) by solvent evaporation
166 using a rotary evaporator (Heidolph Instruments GmbH & CO). Rehydration of the lipid film with
167 phosphate buffer (pH=7.4) produced SUVs. The SUVs were then homogenized and brought to the
168 desired size (≤ 200 nm) by extrusion through Avanti mini-Extruder (Avanti Polar Lipids, USA)
169 containing a polycarbonate membrane with a pore size of 200 nm. The SDS micelles were simply
170 prepared by dissolving SDS powder in Milli-Q water at a concentration of 25 mM. The size of the
171 lipid vesicles was measured by Dynamic light scattering (ZetaPALS, Brookhaven instruments
172 corporation) and reported as the average of 6 scans.

173 Surface activity and interaction of the peptides with lipid monolayers

174 The surface pressure measurements were performed using a Langmuir trough (NIMA technology
175 Ltd, Coventry, UK), with a 3 ml built-in Teflon trough filled with PBS (pH=7.4) and a Wilhelmy plate
176 attached to the pressure sensor. The peptide solution at different concentrations (10-40 μ M) was
177 injected underneath the buffer surface using a Hamilton microsyringe and the changes to the surface
178 pressure at the air-water interface were recorded as a function of time for 2 h. The surface pressure
179 was obtained by calculating the difference between the initial surface tension of the pure water and
180 the final surface tension following adsorption of the peptides at the air/water interface:

$$181 \quad \pi = \gamma_0 - \gamma \quad \text{Eq. 3.}$$

182 Where π is the surface pressure, γ_0 is the initial surface tension of pure water and γ is the final surface
183 tension ^{41, 70}.

184 The interaction of the peptides with the lipid monolayers was studied by monitoring the changes
185 to the surface pressure of DPPG and DPPC lipid monolayers upon contact with the peptide solution.
186 The lipid monolayers were formed by spreading the lipid solution in chloroform (0.5 mg/mL) at the
187 air-buffer interface using a Hamilton microsyringe and allowing for the solvent to evaporate (20 min).
188 The peptide solution was injected into the subphase (at a final concentration of 20 μ M) and the
189 changes to the surface pressure over time were monitored for 2 h. The initial pressure of the lipid
190 monolayer was set to 28 mN/m which is close to the average cell membrane resting pressure ^{61, 62,}
191 ⁷¹. All the measurements were performed in triplicate and the values were reported as the average
192 of the three repeats.

193 Cytotoxicity tests

194 The cytotoxicity tests were performed in three different cell lines: HCT 116 colorectal
195 adenocarcinoma cells, HeLa cervical cancer cells, and Human dermal fibroblasts (HDFs). The cells

196 were cultured in DMEM enriched with 10% FBS and 1% antibiotic (100 U/mL penicillin and 100
197 $\mu\text{g/mL}$ streptomycin) at 37 °C under 5% CO₂. For the cytotoxicity tests, the cells were cultured in 96
198 well plates at a seeding density of 4000 cells/well and incubated with different concentrations of the
199 peptide solutions for 72 h. The cell viability was assessed by MTT assay following standard protocols.
200 Briefly, 10 μL of 3-(4,5-dimethylthiazol-2-yl)-2,5-diphenyltetrazolium bromide (MTT) solution (5
201 mg/mL) was added to each well and incubated at 37 °C for 4 h. Subsequently, the media was
202 removed and replaced with Dimethyl Sulfoxide (DMSO). The plates were shaken for 15 min to allow
203 for complete dissolution of the formazan dye and then the absorbance of formazan at 590 nm was
204 measured using a microplate reader (Varioskan Flash™, Thermo Fisher Scientific). The relative cell
205 viability was determined with respect to the untreated controls. All experiments were repeated 6
206 times and the values were reported as Mean \pm SE of the 6 replicates.

207 Mitochondrial damage tests

208 The ability of the designed anticancer peptides to damage the mitochondrial membrane was
209 evaluated using JC-1 mitochondrial probe. The cells were cultured in 96 well plates at a seeding
210 density of 4000 cells/well and incubated with the peptide solutions (at the concentration of 20 μM).
211 After 72 h, the cells were stained with JC-1 following the manufacturer's protocol. Briefly, the cells
212 were washed with PBS, immersed in fresh media containing JC-1 (10 $\mu\text{g/mL}$) and incubated at 37
213 °C for 15 min. Subsequently, the media was removed, the cells were washed with PBS, submerged
214 in PBS and imaged with high content fluorescent automated widefield microscope (ImageXpress®
215 Micro System, Molecular Devices, USA).

216 Data analysis

217 The quantitative data were analysed using Microsoft® Excel 2016 and GraphPad Prism 9. All
218 data were reported Mean \pm SE of the repeats. For the correlation graphs the data were subjected to
219 linear regression analysis at 95% confidence interval ($\alpha = 0.05$) and values of $p < 0.05$ were used to
220 determine the goodness of fit. The microscopic images were analysed using MetaXpress® software
221 5.3.01 (Molecular Devices, USA).

222 3. Results and discussion

223 Structure and physicochemical properties of the peptides

224 The molecular weights measured by LC-MS were similar to the theoretical molecular weights
225 calculated using the online software which confirms the peptide sequences (**Table 1**). Comparing
226 the values of mean residue hydrophobicity of different peptides in this series indicated that there was
227 no significant difference between the hydrophobicities of the peptides that contained the same type
228 of amino acid in their hydrophobic domain, but the isoleucine-rich peptides had slightly higher
229 hydrophobicity than the leucine-rich counterparts. Changing the hydrophilic amino acids (arginine or
230 lysine) in the peptide sequence seemed to have a minimal effect on their mean residue

231 hydrophobicity. On the contrary, the apparent hydrophobicities determined by RP-HPLC retention
 232 times revealed a different trend for hydrophobicity in this series of peptides. The leucine-rich peptides
 233 were more hydrophobic than the isoleucine-rich peptides and there was a significant increase in
 234 hydrophobicity by replacing the lysine residues with arginine residues. These observations further
 235 confirm the previously reported claims that the hydrophobicity of a peptide is not only a function of
 236 its amino acid composition or polarity but is also influenced by other factors such as peptide
 237 secondary structure. Therefore, the RP-HPLC retention time provides a more accurate measure of
 238 the peptide hydrophobicity than the mean residue hydrophobicity as it reflects the real-time
 239 interaction of the peptide with the hydrophobic surface of the HPLC stationary phase ^{41, 68, 72, 73}.

240

241 **Table 1.** Sequences and physicochemical properties of the designed β -sheet forming anticancer peptides.

Peptide	Sequence	Charge	Theoretical MW ^a	Measured MW ^b	RT ^c	<H> ^d
IKIK	IKIKIKIKIKI-NH ₂	+6	1464.10	1464.12	8.6	0.405
LKLK	LKLKLLKLKLK-NH ₂	+6	1464.10	1464.12	8.9	0.355
IKIR	IKIRIKIRIKIR-NH ₂	+6	1548.12	1548.14	8.8	0.400
LKLR	LKLRLKLRLKLR-NH ₂	+6	1548.12	1548.14	9.2	0.350
IRIK	IRIKIRIKIRIK-NH ₂	+6	1548.12	1548.14	8.8	0.400
LRLK	LRLKLRLKLRLK-NH ₂	+6	1548.12	1548.14	9.2	0.350
LRLR	LRLRLRLRLRLR-NH ₂	+6	1632.14	1632.16	9.5	0.345

242 a Theoretical molecular weights calculated using the online tool from the website "<https://pep-calc.com>"; b Experimental molecular weights
 243 measured by LC-MS; c HPLC retention times; d Mean residue hydrophobicity calculated by Eisenberg method using the hydrophobicity
 244 scale defined by Fauchère and Pliska.

245

246 Secondary structure of the peptides

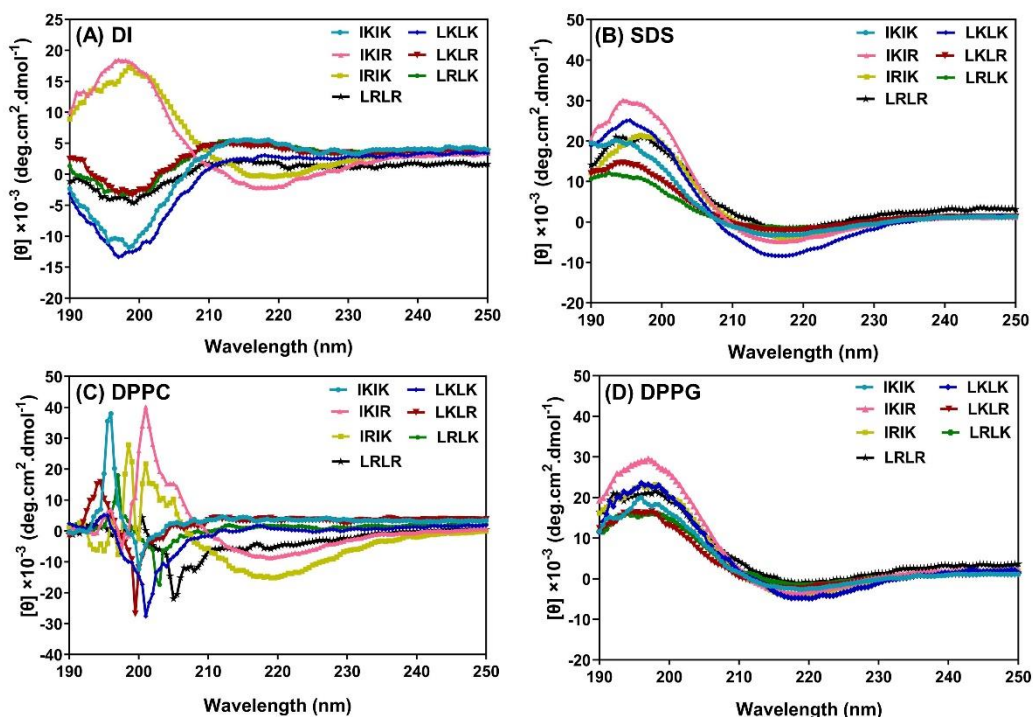
247 The secondary structure of the designed anticancer peptides in different environments as
 248 determined by circular dichroism (CD) spectroscopy are presented in **Figure 1**. All peptides except
 249 IKIR and IRIK had an unfolded random coil structure in the aqueous solution as indicated by a
 250 negative peak at near 198-200 nm ^{49, 50, 74}. This is supposed to be because of the electrostatic
 251 repulsion between the positively charged arginine/lysine residues within the peptide molecules ⁴⁹.
 252 IKIR and IRIK on the other hand, exhibited β -sheet structures indicated by a positive peak at 197-
 253 200 nm and a negative peak at 217-218 nm ^{49, 50, 53}. The different behaviour of IKIR and IRIK
 254 compared to the rest of the peptides in this series is suggested to result from the interplay between
 255 the electrostatic parameter and the other pertinent factors which contribute to the peptide folding in
 256 aqueous media including steric parameter, hydrophobic parameter, amino acid side chain density,
 257 amino acid nonpolar accessible surface area, and overall amino acid packing density ⁷⁵⁻⁸⁰. The steric
 258 parameter which reflects the bulk and branching of the amino acid side chains influences the
 259 rotational flexibility of the peptide chain and consequently its likelihood to fold into β -sheet
 260 conformation in aqueous solution ^{77, 78}. I has higher steric parameter than L and therefore the
 261 peptides containing I are more likely to form β -sheet structures than the peptides containing L ^{77, 78}.
 262 Similarly, the overall side chain density of the amino acids in the peptide sequence affects the

263 rotational flexibility of the peptide and the combination of amino acids in IRIK/IKIR has lower overall
264 side chain density compared to their leucine bearing counter parts and also compared to IKIK which
265 bestows higher rotational flexibility upon these two peptides^{75,80}. The higher hydrophobicity reported
266 for R compared to K in several hydrophobicity scales such as the Wimley White hydrophobicity scale
267⁷⁵ and the Dwyer inverted hydrophobicity scale⁷⁷ further justifies the higher propensity of IRIK and
268 IKIR for forming β -sheet conformation compared to IKIK as it has been evidenced that the higher
269 hydrophobicity of amino acids increases their preference for forming β -sheet structures⁷⁷.
270 Furthermore, the lower overall accessible surface area^{75,76} and the higher overall residue packing
271 density⁷⁹ for IKIR and IRIK compared to the other peptides in this series also justifies the formation
272 of β -sheet structures by these two peptides in aqueous solution while other peptides in this group
273 remain unfolded. The accessible surface area and the packing density of amino acids in a peptide
274 or protein sequence are considered as predictors of folding of peptides and proteins^{75,76,79}.

275 Unlike the aqueous solution in the anionic environment of SDS micelles and DPPG SUVs all
276 peptides adopted β -sheet structures denoted by a positive peak at 197-200 nm and a negative peak
277 at 217-218 nm^{49,50,53}. This conformational change is supposed to happen as a result of the
278 electrostatic interaction between the positively charged arginine/lysine residues of the peptides and
279 the negatively charged SDS/DPPG headgroups followed by interaction of the hydrophobic residues
280 of the peptide with the hydrophobic tail of the SDS/DPPG^{49,53}. In the zwitterionic environment of
281 DPPC SUVs, on the other hand, the peptides showed a combination of random coil structure and β -
282 sheet structure, indicated by a positive peak at 194-200 nm and a negative peak at 200-205 nm.
283 This could be indicative of some regions of the peptide adopting β -sheet conformation while the
284 other regions remaining unfolded. Alternatively, this could result from partial penetration of some
285 peptide molecules into the DPPC lipid bilayer leading to β -sheet formation while the other peptide
286 molecules still exist in random coil structure in the aqueous phase of the SUVs. Similar observations
287 were reported for the antimicrobial peptide arenicin which had a mixture of β -sheet and random coil
288 structure in the micelles of non-ionic surfactant octyl- β -D-glucopyranoside (OG)⁵³.

289 These findings are in accordance with the results from other studies with β -sheet forming
290 antimicrobial peptides with closely related structures. For example, Ong et al⁴⁹ developed short
291 cationic antimicrobial peptides consisting of arginine or lysine in their hydrophilic domain and valine,
292 isoleucine, phenylalanine or tryptophan in their hydrophobic domain. The peptides had a random
293 coil structure in water but transformed into β -sheet structure in SDS micelles⁴⁹. Similar observations
294 have been reported for some of the cell penetrating peptides including penetratin, MPG, and M918
295 which had random coil structure in water and zwitterionic DOPC vesicles but folded into β -sheet
296 structure in anionic DOPG phospholipid vesicles⁷⁴. Unlike the rest of the peptides, IKIR and IRIK
297 exhibited β -sheet structure both in the anionic environments and in the neutral or zwitterionic
298 environments. Nonetheless, they possessed a less defined β -sheet conformation in DPPC SUVs
299 compared to DPPG SUVs and SDS micelles. This suggests that the presence of isoleucine residues
300 in the hydrophobic domain of the peptide is more favourable for β -sheet formation than leucine

301 residues. Moreover, the combination of lysine and arginine residues in the hydrophilic domain of the
302 peptide enhances the tendency for β -sheet conformation than either arginine or lysine alone.
303

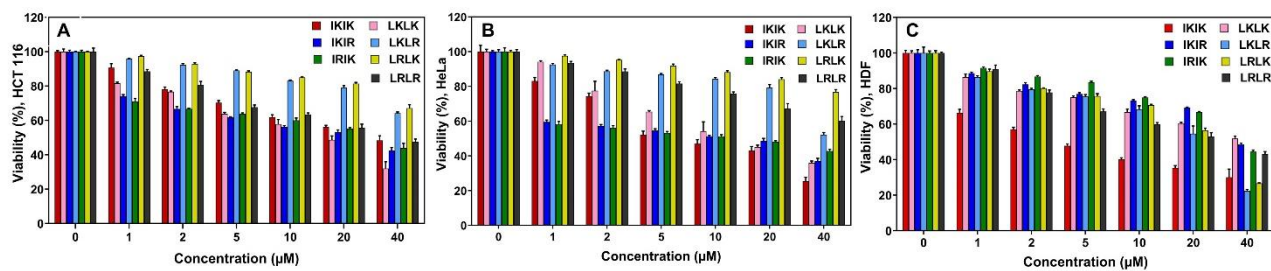


304
305 **Figure 1.** Circular dichroism (CD) spectra of the cationic amphiphilic peptides in DI water (A), SDS micelles
306 (B), DPPC SUVs (C) and DPPG SUVs (D).

307 308 Cytotoxicity of the peptides in normal and cancer cells

309 The cytotoxicity of the designed anticancer peptides as determined by MTT assay is depicted in
310 **Figure 2** and the values of half maximal inhibitory concentration (IC_{50}) of the peptides in different
311 cell lines are presented in **Table 2**. As it could be inferred from these data, LKLR was the most toxic
312 peptide in HCT 116, with the highest efficacy and potency in the experimental concentration range
313 ($IC_{50} = 14.5 \pm 1.3 \mu\text{M}$ and $68.1 \pm 2.1 \%$ growth inhibition). Replacing the leucine residues of this
314 peptide with isoleucine residues (IKIK) or replacing the lysine residues with arginine residues (LKLR
315 and LRLK and LRLR) resulted in considerable decrease in anticancer activity against HCT 116
316 compared to LKLR as evidenced by the higher values of IC_{50} for these peptides. IKIR also showed
317 considerable toxicity in HCT 116 cells whereas its leucine containing analogue, LKLR did not show
318 significant toxicity against HCT 116 in the experimental range of concentrations.

319



320

321 **Figure 2.** Cytotoxicity of the designed anticancer peptides in HCT 116 (A), HeLa (B), and HDF (C) as
 322 determined by MTT assay. All values were normalized compared to the untreated controls and reported as
 323 Mean \pm SE of 6 repeats.

324

325 **Table 2.** Half maximal inhibitory concentrations (IC_{50}) of the designed anticancer peptides in different cell lines
 326 as determined by MTT assay. All values are reported as Mean \pm SD of 6 replicates.

Peptide	IC_{50} (μ M)		
	HCT 116	HeLa	HDF
IKIK	32.7 \pm 4.5	8.9 \pm 2.1	4.4 \pm 0.3
LKLR	14.5 \pm 1.3	17.7 \pm 6.5	> 40
IKIR	20.9 \pm 2.0	14.5 \pm 2.3	38.6 \pm 0.2
LKLR	> 40	> 40	22.5 \pm 1.4
IRIK	30.1 \pm 5.2	15.5 \pm 1.2	34.5 \pm 0.9
LRLK	> 40	> 40	24.1 \pm 0.7
LRLR	31.8 \pm 2.9	> 40	22.7 \pm 2.4

327

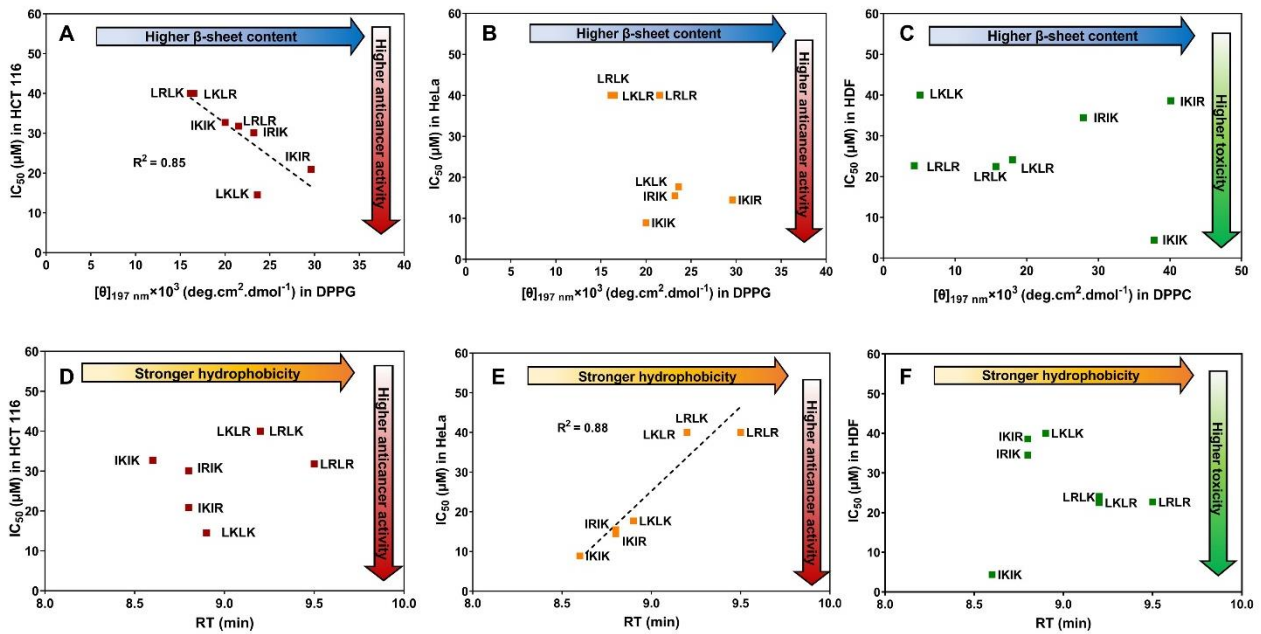
328 In HeLa cells, on the other hand, IKIK was the most toxic peptide (IC_{50} = 8.9 \pm 2.1 μ M and 74.4
 329 \pm 1.4 % growth inhibition). LKLR, IRIK, and IKIR were also highly toxic to HeLa cells without any
 330 significant difference between them. The rest of the peptides did not exhibit any cytotoxicity against
 331 HeLa cells. In contrast to the trend observed for cytotoxicity in cancer cells, in HDF cells the peptides
 332 containing leucine in their hydrophobic domain and arginine in their hydrophilic domain (LRLR, LRLK,
 333 and LKLR) exhibited considerable cytotoxicity, whereas LKLR and IKIR had minimal toxicity against
 334 HDFs. IKIK also exhibited high toxicity against fibroblasts which was comparable to its toxicity
 335 against HeLa cells.

336 As it could be inferred from these data, the combination of leucine and arginine diminishes the
 337 anticancer activity of the peptides but renders them more toxic to HDFs. Overall, LKLR, IKIR, and
 338 IRIK possessed selective anticancer activity with low toxicity against HDFs. LKLR was equally toxic
 339 to HCT 116 and HeLa cells, while IKIR and IRIK favoured HeLa cells over HCT 116 cells. These
 340 data indicate the importance of testing the anticancer peptides in different cancer cell lines to
 341 investigate cancer-specific cytotoxicity. This could help in rational design of peptides with enhanced
 342 cytotoxicity against specific cancers and with reduced cytotoxicity against normal tissues. It is also
 343 noteworthy that the cell viability tests were performed in media enriched with FBS. Hence, the high
 344 anticancer activity of the peptides in the presence of FBS indicates their resistance to serum
 345 proteases.

346 Cytotoxicity of the peptides is influenced by their secondary structure and their 347 hydrophobicity

348 The relationship between cytotoxicity of the peptides in different cell lines, their secondary
349 structure in phospholipid vesicles and their hydrophobicity is depicted in **Figure 3**. The values of
350 mean residue molar ellipticity at 197-200 nm were used to compare the β -sheet content of the
351 different peptides^{50, 53} and the RP-HPLC retention times were used as a measure of hydrophobicity
352^{41, 68, 72, 73}. There was a strong correlation between the β -sheet content of the peptides in negatively
353 charged DPPG SUVs and their anticancer activity in HCT 116 cells which suggests the same
354 conformational changes from random coil to β -sheet may take place in the cell membrane of HCT
355 116 cells. On the other hand, no direct relationship was found between the β -sheet content of the
356 peptides in DPPG SUVs and their anticancer activity against HeLa cells. Contrastingly, the
357 anticancer activity of the peptides in HeLa cells was inversely proportional to their hydrophobicity
358 whereas no direct relationship between the anticancer activity of the peptides in HCT 116 cells and
359 their hydrophobicity was found. It could be inferred from these data that the cytotoxicity of the
360 peptides against HCT 116 cells is more influenced by their secondary structure upon contact with
361 cancer cell membranes whereas their cytotoxicity against HeLa cells is more directed by their
362 hydrophobicity. Hence, the anticancer activity of the peptides is directed by an interplay between
363 their secondary structure and their hydrophobicity.

364 Lack of a good correlation between the cytotoxicity of the peptides in HDF cells and their β -sheet
365 content in zwitterionic DPPC SUVs suggests that the conformational changes upon interaction of
366 the peptides with the normal cell membranes don't play a significant role in their cytotoxicity against
367 normal cells. The only exception is IKIK which had a very high β -sheet content in DPPC SUVs and
368 exhibited the highest toxicity against HDF cells among all of the peptides. This may be in part due to
369 the presence of a mixture of β -sheet and random coil structures in these peptides in the zwitterionic
370 lipid bilayers which reduces their penetration into the cell membrane compared to the complete β -
371 sheet structure formed in anionic lipid bilayers as discussed earlier. On the other hand, with the
372 exception of IKIK, the cytotoxicity of the peptides against HDF cells was directly proportional to their
373 hydrophobicity and the most hydrophobic peptides were the most toxic. Hence, the cytotoxicity of
374 the peptides against normal cells is mainly influenced by their hydrophobicity and the β -sheet
375 secondary structure does not play an important role in it.



376

377 **Figure 3.** Relationship between the anticancer activity of the peptides in HCT 116 (A) and HeLa (B) and their
 378 β-sheet content in DPPG small unilamellar vesicles (SUVs). (C) Relationship between the cytotoxicity of the
 379 peptides in HDF and their β-sheet content in DPPC SUVs. Relationship between the hydrophobicity of the
 380 peptides and their cytotoxicity in HCT 116 (D), HeLa (E), and HDF (F).

381

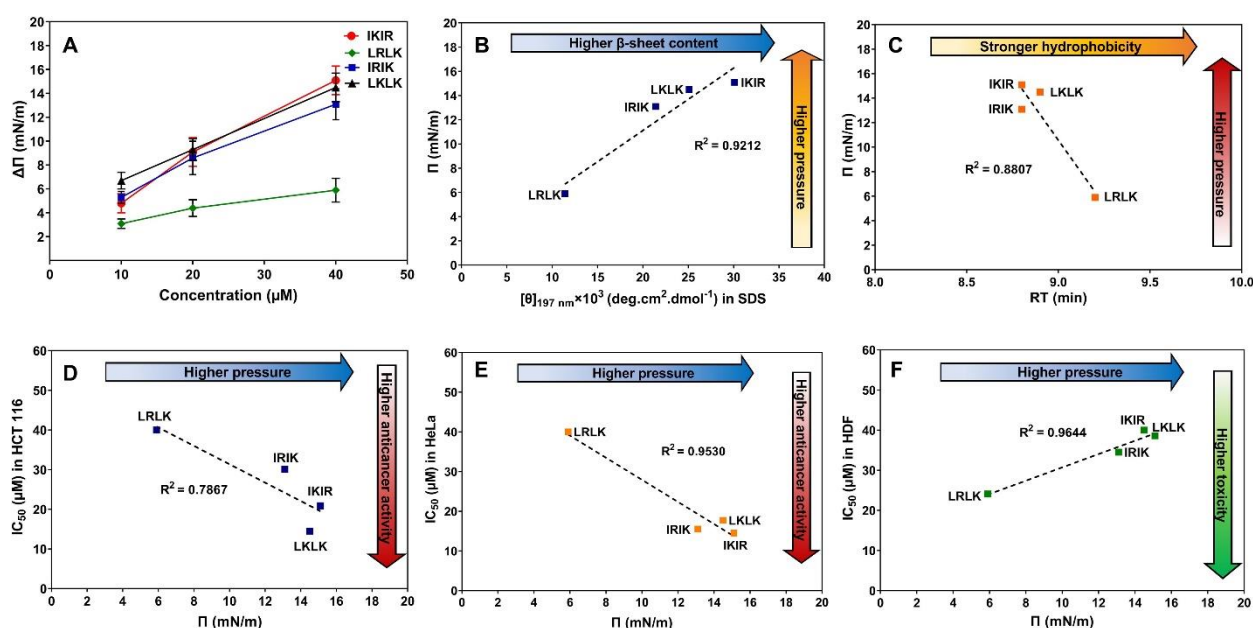
382 Surface activity of the peptides determines their anticancer activity

383 The amphiphilicity of the designed anticancer peptides was measured by their surface pressure
 384 at the air-water interface which serves as a good model for a hydrophobic/hydrophilic interface⁷⁴.
 385 Three peptides (IKIR, IRIK and LKLK) with higher selectivity for cancer cells were studied and one
 386 peptide (LRLK) with poor anticancer activity and high toxicity in fibroblast was used as a negative
 387 control. Changes to the surface tension of pure water upon adsorption of the peptide molecules at
 388 the air-water interface, referred to as “surface pressure”, is indicative of the surface activity of a given
 389 peptide^{40, 41}. As it could be observed in **Figure 4A**, there was an increase in the surface pressure
 390 upon injection of the anticancer peptides at the air-water interface which indicates the surface activity
 391 of the designed anticancer peptides. Increasing the concentration of the peptide in the subphase
 392 resulted in higher surface pressure indicating that the interfacial adsorption of the peptides is
 393 concentration dependent.

394 The surface pressure of the peptides was directly proportional to their β-sheet content in SDS
 395 micelles (**Figure 4B**) and inversely proportional to their hydrophobicity (**Figure 4C**). This observation
 396 suggests the same conformational changes that happen at the oil-water interface of the SDS
 397 micelles may also take place upon adsorption of the peptides at the air-water interface to allow for
 398 insertion of the polar surface of the β-sheet into the subphase and projection of the hydrophobic
 399 surface of the β-sheet outside the water in the air to achieve the most stable (lowest energy) status.
 400 A conformational change from random coil to β-sheet structure has been reported by Maget-Dana
 401 et al⁸¹ for a cationic amphiphilic peptide consisting of Leucine and Lysine residues, (LK)₅₀, upon

402 forming a peptide monolayer on the surface of water ^{70, 81}. The adverse effect of increased
 403 hydrophobicity on the surface activity suggests the importance of the hydrophobic-hydrophilic
 404 balance (i.e., amphiphilicity) for the optimal surface activity of the peptides. Thus, the surface activity
 405 of the cationic amphiphilic peptides is directed by an interplay between their hydrophobicity and their
 406 secondary structure.

407 There was a direct relationship between the surface pressure of the peptides and their anticancer
 408 activity (**Figure 4D-E**) while the toxicity of the peptides in HDFs was inversely proportional to their
 409 surface activity (**Figure 4F**). These findings suggest that the surface activity of the peptides has a
 410 determining role in their anticancer activity and toxicity to normal cells. Although there is no literature
 411 data on the surface activity of the β -sheet forming ACPs, the influence of the surface activity of the
 412 peptides on their antimicrobial or anticancer activity has been reported for some α -helical AMPs and
 413 ACPs ^{40, 41, 62}, in which the biological activity was a function of the surface activity. Hence, measuring
 414 the surface activity can provide a tool for predicting the biological activity of this class of cationic
 415 amphiphilic peptides and modifying the peptide design accordingly to achieve higher anticancer
 416 activity.

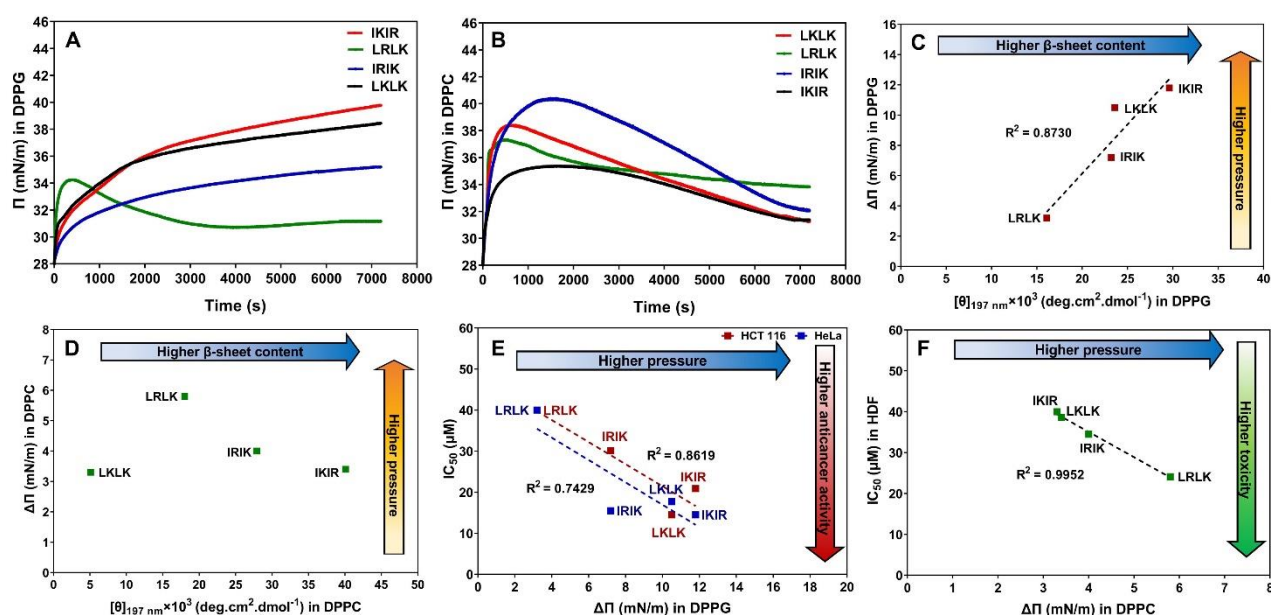


417
 418 **Figure 4.** Increase in surface pressure at the air-water interface following injection of different concentrations
 419 of the anticancer peptides (**A**). Correlation between the surface pressure of the cationic amphiphilic peptides
 420 and their β -sheet content in SDS micelles (**B**). Correlation between the surface pressure of the cationic
 421 amphiphilic peptides and their hydrophobicity (**C**). Correlation between the cytotoxicity of the peptides in HCT
 422 116 (**D**), HeLa (**E**), HDF (**F**) and increase in surface pressure upon adsorption of the peptides (40 μM) at the
 423 air-water interface.

424 425 Penetration of the anticancer peptides into phospholipid monolayers reveals their 426 mechanism of cell selectivity

427 As mentioned previously, it is widely accepted that the higher selectivity of the ACPs for cancer
 428 cells compared to normal cells is due to their higher tendency for interaction with the anionic cancer

429 cell membranes compared to the zwitterionic normal cell membranes^{32-37, 39}. In order to investigate
 430 the interaction of our designed anticancer peptides with different types of cell membranes, negatively
 431 charged DPPG lipid monolayers and zwitterionic DPPC lipid monolayers were used as a model for
 432 the outer leaflet of the cancer cell and normal cell membrane respectively^{61, 71, 82}. The increase in
 433 the surface pressure of the lipid monolayer upon injection of the peptide solution in the subphase at
 434 a constant surface area is indicative of peptide insertion into the lipid monolayer^{61, 62, 71}.
 435



436

437 **Figure 5.** Increase in the pressure of the DPPG (A) and DPPC (B) lipid monolayers upon injection of the
 438 anticancer peptides (20 μM) in the subphase. Correlation between the β -sheet content of the peptides in DPPG
 439 SUVs and increase in the surface pressure of DPPG monolayers (C). Correlation between the β -sheet content
 440 of the peptides in DPPC SUVs and increase in the surface pressure of DPPC monolayers (D). Correlation
 441 between cytotoxicity of the peptides in cancer cells and increase in the surface pressure of DPPG lipid
 442 monolayers (E). Correlation between cytotoxicity of the peptides in HDF and increase in the surface pressure
 443 of DPPC lipid monolayer (F).

444

445 The changes to the surface pressure following injection of the anticancer peptides under DPPG
 446 and DPPC monolayers are presented in **Figure 5A-B**. Three peptides with highest anticancer activity
 447 and highest selectivity for cancer cells (IKIR, IRIK, and LKLK) and one peptide with poor anticancer
 448 activity and no selectivity for cancer cells (LRLK) were included in these experiments for comparison.
 449 As it is evident from these plots, the anticancer peptides which were more selective for cancer cells
 450 than fibroblasts (IKIR, IRIK, and LKLK) had considerably higher affinity for DPPG lipid monolayers
 451 than DPPC lipid monolayers and penetrated more into DPPG monolayers. On the other hand, LRLK
 452 which lacked toxicity against cancer cells and was toxic to fibroblasts penetrated into DPPC lipid
 453 monolayers more than DPPG monolayers and more than the other peptides (**Figure 5B**). These
 454 data confirm that the higher selectivity of the designed anticancer peptides for cancer cells results
 455 from their higher affinity for cancer cell membranes and greater penetration into the cancer cell
 456 membranes. Similar results were reported for the β -sheet forming cell penetrating peptide M918

457 which exhibited higher affinity for the anionic DOPG lipid monolayer compared to the zwitterionic
458 DOPC lipid monolayer⁸³. Also the linear form of the antimicrobial peptide arenicin showed higher
459 affinity for DPPG lipid monolayers than DPPC lipid monolayers whereas its cyclic analogue which
460 was highly toxic to human erythrocytes showed higher affinity for DPPC monolayers⁵³. These
461 findings suggest the lipid monolayers as a suitable *in vitro* model for studying the interaction of the
462 anticancer peptides with the cell membranes and predicting their cytotoxicity against normal and
463 cancer cells. The suggested biophysical method could be used as powerful tool for pre-screening
464 the newly designed anticancer peptides prior to performing the costly cell-based screening.

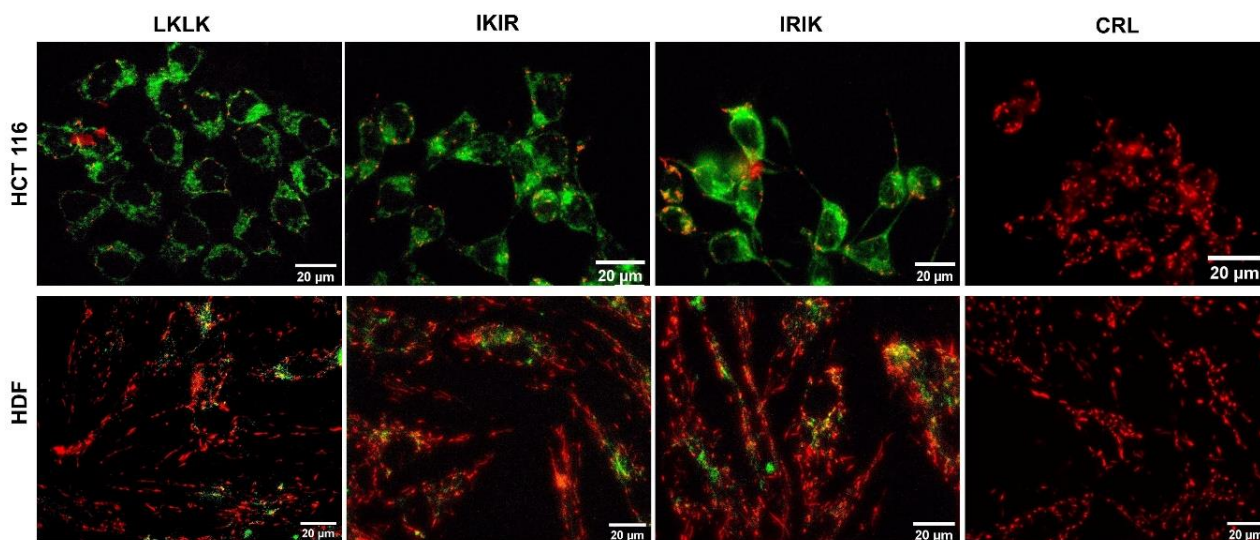
465 The increase in surface pressure of DPPG monolayers following insertion of the peptides was
466 well correlated to the β -sheet content of the peptides in DPPG SUVs (Figure 5C) suggesting that
467 the same conformational changes from random coil to β -sheet that occur upon interaction of the
468 peptides with the lipid bilayer of DPPG SUVs may also occur upon interaction of the peptides with
469 the DPPG lipid monolayers. Conformational change from random coil to β -sheet upon interaction
470 with DPPG monolayers has been previously demonstrated for the linear analogue of arenicin using
471 Infrared reflection absorption spectroscopy (IRRAS)⁵³. It is assumed that the electrostatic interaction
472 between the positively charged arginine and lysine residues of the peptides and the negatively
473 charged headgroups of the phospholipids provides initial binding of the peptide to the surface of the
474 lipid monolayer. Subsequently, the peptide transforms from random coil structure into β -sheet
475 structure with separate hydrophobic and hydrophilic surfaces. This conformational change allows for
476 hydrophobic interactions between the isoleucine and leucine residues in the hydrophobic surface of
477 the peptide and the acyl chains of the phospholipids which disturbs the acyl chain ordering of the
478 lipid monolayer manifested by an increase in surface pressure. The suggested molecular mechanism
479 of peptide penetration into lipid monolayers has also been reported for other types of lysine and
480 leucine-based peptides^{81, 84}. On the other hand, lack of good correlation between the secondary
481 structure in DPPC SUVs and the pressure increase in DPPC lipid monolayers (Figure 5D) suggests
482 that penetration of the designed ACPs into zwitterionic DPPC monolayers is mainly a result of
483 hydrophobic interactions between the hydrophobic amino acid residues of the peptide and the acyl
484 chains of DPPC.

485 There was a good correlation between the anticancer activity of the peptides in HCT 116 and
486 HeLa and the increase in surface pressure of the DPPG monolayers induced by them (Figure 5E).
487 In a similar fashion, the increase in surface pressure of DPPC monolayers upon injection of the
488 anticancer peptides was strongly correlated to their toxicity in HDF cells (Figure 5F). These data
489 further confirm that the selectivity of the anticancer peptides for cancer cells results from higher
490 penetration into the cancer cell membranes compared to normal cell membranes presumably due to
491 the difference in their surface charge.

492

493 The anticancer peptides exert their cytotoxicity by damaging the mitochondria

494 Interaction of the designed anticancer peptides with the mitochondrial membranes was
495 investigated by assessing the mitochondrial membrane depolarization following treatment with the
496 peptides. The high content images of HCT 116 and HDF cells stained with JC-1 after treatment with
497 the anticancer peptides LKLK, IKIR, and IRIK are presented in **Figure 6**. These three peptides were
498 selected for this experiment due to their higher selectivity for cancer cells compared to fibroblasts.
499 JC-1 is a mitochondrial probe and its accumulation in the mitochondria depends only on the
500 mitochondrial membrane potential^{85,86}. While the accumulation of JC-1 in healthy mitochondria gives
501 rise to red fluorescence, depolarization of the mitochondrial membranes in pre-apoptotic cells results
502 in reduced accumulation of JC-1 indicated by a shift from red to green fluorescence^{87,88}. Hence, the
503 higher proportion of green to red fluorescence observed in HCT 116 after treatment with the
504 anticancer peptides denotes damage to the mitochondrial membrane whereas higher red to green
505 fluorescence ratio in HDF cells indicates less damage to the mitochondria. This is consistent with
506 the literature data reporting mitochondrial membrane disruption as one of the common mechanisms
507 of action for anticancer peptides^{32, 34, 35, 37, 39}. The high affinity of the anticancer peptides for
508 mitochondrial membrane is attributed to its high content of anionic lipids such as cardiolipin^{32, 34, 35,}
509 ^{37, 39}.



510

511 **Figure 6.** Mitochondrial membrane depolarization by the anticancer peptides in HCT 116 (**top panel**) and HDF
512 cells (**bottom panel**) as determined by JC-1 mitochondrial probe. The red fluorescence indicates healthy
513 mitochondria, and the green fluorescence indicates damaged mitochondria in pre-apoptotic cells.

514

515 Conclusion

516 Herein, we report the development of a new series of β -sheet forming anticancer peptides and
517 their structure activity relationship. The secondary structure of the peptides before and after
518 interaction with model membranes was studied by CD spectroscopy and their surface activity at the

519 air-water interface as well as their penetration into model lipid monolayers was studied using
520 Langmuir-tensiometer. Some of our designed peptides had higher toxicity to cancer cells compared
521 to fibroblasts and some had a stronger anticancer effect against HeLa cervical cancer cells
522 compared to HCT 116 colorectal cancer cells. It has been found that the best combination of amino
523 acids for achieving high anticancer activity against HCT 116 is the combination of leucine and lysine
524 (LKLK) whereas in HeLa cells the most toxic peptide was IKIK although IKIR, IRIK, and LKLK were
525 all very toxic to HeLa. These observations suggest that in addition to general toxicity to cancer cells,
526 this class of peptides possess some cancer cell specific cytotoxicity. On the other hand, the peptides
527 consisting of leucine in their hydrophobic domain and arginine in their hydrophilic domain (LRLR,
528 LRLK, and LKRL) had considerable toxicity against fibroblast cells and which is not favourable.
529 Hence, this combination of amino acids is not recommended for the β -sheet forming cationic
530 amphiphilic anticancer peptides. The anticancer activity of the peptides was found to be strongly
531 correlated with their secondary structure, their amphiphilicity and surface activity. This has also been
532 reported for other types of short cationic amphiphilic antimicrobial and anticancer peptides with α -
533 helical structure^{40, 41, 61, 62, 89}. The higher selectivity of the peptides for cancer cells was found to be
534 a result of their higher affinity for the negatively charged membranes compared to zwitterionic
535 membranes as revealed by higher penetration of the peptides into negatively charged lipid
536 monolayers. This has been generally accepted as one of the main mechanisms of cell selectivity for
537 anticancer peptides^{32-37, 39}. The peptides exerted their anticancer activity by damaging the
538 mitochondrial membranes leading to apoptosis, which has been widely reported as one of the main
539 mechanisms of cytotoxicity for many anticancer peptides^{32, 34, 35, 37, 39}. The results from this study
540 serve as a guide for the structure-activity relationship of this class of anticancer peptides and will
541 contribute to the development of anticancer peptides with enhanced efficacy and selectivity. Future
542 work is mainly directed towards improvement of the structural design for this type of peptides to
543 enhance their anticancer activity and broaden their anticancer spectrum. Investigating the peptide
544 aggregation into higher ordered structures in membrane environments, the structural features of
545 such aggregates and the exact mechanism of cell membrane disruption by the peptides (i.e., carpet,
546 barrel and stove, toroidal pore, etc.) is also another area to be covered by future studies.

547 CRediT authorship contributions statement

548 RH: Conceptualization, Methodology, Investigation, Validation, Formal analysis, Data curation,
549 Visualization, Writing - Original Draft; MAT: Methodology, Writing - Review & Editing; SB:
550 Supervision; JW: Resources; XZ: Conceptualization, Methodology, Visualization, Writing - Review &
551 Editing, Supervision, Project administration, Funding acquisition.

552 Declaration of Competing Interest

553 The authors declare that they have no known competing financial interests or personal
554 relationships that could have appeared to influence the work reported in this paper.

555 Acknowledgements

556 The authors would like to thank EPSRC (EP/N007174/1 and EP/N023579/1), Royal Society
557 (RG160662 and IE150457) and Jiangsu specially appointed professor program for support. The
558 authors would also like to thank Dr Caroline Evans from the Department of Chemical and Biological
559 Engineering, University of Sheffield and Mr Rob Hanson from the Department of Chemistry,
560 University of Sheffield for their technical assistance. RH would like to thank the University of Sheffield
561 for scholarship.

563 4. References

- 564 1. Stratton, M. R.; Campbell, P. J.; Futreal, P. A., The cancer genome. *Nature* **2009**, *458* (7239), 719-724.
565 2. Martínez-Jiménez, F.; Muiños, F.; Sentís, I.; Deu-Pons, J.; Reyes-Salazar, I.; Arnedo-Pac, C.; Mularoni,
566 L.; Pich, O.; Bonet, J.; Kranas, H.; Gonzalez-Perez, A.; Lopez-Bigas, N., A compendium of mutational cancer
567 driver genes. *Nature Reviews Cancer* **2020**, *20* (10), 555-572.
568 3. Chen, D. S.; Mellman, I., Elements of cancer immunity and the cancer-immune set point. *Nature* **2017**,
569 *541* (7637), 321-330.
570 4. Hanahan, D.; Weinberg, Robert A., Hallmarks of Cancer: The Next Generation. *Cell* **2011**, *144* (5), 646-
571 674.
572 5. Galmarini, D.; Galmarini, C. M.; Galmarini, F. C., Cancer chemotherapy: A critical analysis of its 60 years
573 of history. *Critical Reviews in Oncology/Hematology* **2012**, *84* (2), 181-199.
574 6. Jhaveri, K. D.; Shah, H. H.; Calderon, K.; Campenot, E. S.; Radhakrishnan, J., Glomerular diseases seen
575 with cancer and chemotherapy: a narrative review. *Kidney International* **2013**, *84* (1), 34-44.
576 7. Tamargo, J.; Caballero, R.; Delpón, E., Cancer Chemotherapy and Cardiac Arrhythmias: A Review. *Drug*
577 *Safety* **2015**, *38* (2), 129-152.
578 8. Lemieux, J.; Maunsell, E.; Provencher, L., Chemotherapy-induced alopecia and effects on quality of life
579 among women with breast cancer: a literature review. *Psycho-Oncology* **2008**, *17* (4), 317-328.
580 9. Reich, M.; Lesur, A.; Perdrizet-Chevallier, C., Depression, quality of life and breast cancer: a review of
581 the literature. *Breast Cancer Research and Treatment* **2008**, *110* (1), 9-17.
582 10. Pollack, J.; Holm, T.; Cedermark, B.; Altman, D.; Holmström, B.; Glimelius, B.; Mellgren, A., Late
583 adverse effects of short - course preoperative radiotherapy in rectal cancer. *British Journal of Surgery*
584 **2006**, *93* (12), 1519-1525.
585 11. Kerns, S. L.; Ostrer, H.; Rosenstein, B. S., Radiogenomics: Using Genetics to Identify Cancer Patients at
586 Risk for Development of Adverse Effects Following Radiotherapy. *Cancer Discovery* **2014**, *4* (2), 155.
587 12. Azria, D.; Ozsahin, M.; Kramar, A.; Peters, S.; Atencio, D. P.; Crompton, N. E. A.; Mornex, F.; Pèlegri,
588 A.; Dubois, J.-B.; Mirimanoff, R.-O.; Rosenstein, B. S., Single Nucleotide Polymorphisms, Apoptosis, and the
589 Development of Severe Late Adverse Effects After Radiotherapy. *Clinical Cancer Research* **2008**, *14* (19),
590 6284.
591 13. Senkus-Konefka, E.; Jassem, J., Cardiovascular effects of breast cancer radiotherapy. *Cancer Treatment*
592 *Reviews* **2007**, *33* (6), 578-593.
593 14. Marine, J.-C.; Dawson, S.-J.; Dawson, M. A., Non-genetic mechanisms of therapeutic resistance in
594 cancer. *Nature Reviews Cancer* **2020**, *20* (12), 743-756.
595 15. Scott, A. M.; Wolchok, J. D.; Old, L. J., Antibody therapy of cancer. *Nature Reviews Cancer* **2012**, *12* (4),
596 278-287.
597 16. Mayes, P. A.; Hance, K. W.; Hoos, A., The promise and challenges of immune agonist antibody
598 development in cancer. *Nature Reviews Drug Discovery* **2018**, *17* (7), 509-527.
599 17. Hahn, A. W.; Gill, D. M.; Pal, S. K.; Agarwal, N., The future of immune checkpoint cancer therapy after
600 PD-1 and CTLA-4. *Immunotherapy* **2017**, *9* (8), 681-692.
601 18. Galluzzi, L.; Humeau, J.; Buqué, A.; Zitvogel, L.; Kroemer, G., Immunostimulation with chemotherapy in
602 the era of immune checkpoint inhibitors. *Nature Reviews Clinical Oncology* **2020**, *17* (12), 725-741.

603 19.Halama, N.; Zoernig, I.; Berthel, A.; Kahlert, C.; Klupp, F.; Suarez-Carmona, M.; Suetterlin, T.; Brand,
604 K.; Krauss, J.; Lasitschka, F.; Lerchl, T.; Luckner-Minden, C.; Ulrich, A.; Koch, M.; Weitz, J.; Schneider, M.;
605 Buechler, M. W.; Zitvogel, L.; Herrmann, T.; Benner, A.; Kunz, C.; Luecke, S.; Springfield, C.; Grabe, N.;
606 Falk, C. S.; Jaeger, D., Tumoral Immune Cell Exploitation in Colorectal Cancer Metastases Can Be Targeted
607 Effectively by Anti-CCR5 Therapy in Cancer Patients. *Cancer Cell* **2016**, *29* (4), 587-601.

608 20.June, C. H., Adoptive T cell therapy for cancer in the clinic. *The Journal of Clinical Investigation* **2007**, *117*
609 (6), 1466-1476.

610 21.Minutolo, N. G.; Hollander, E. E.; Powell, D. J., The Emergence of Universal Immune Receptor T Cell
611 Therapy for Cancer. *Frontiers in Oncology* **2019**, *9*, 176.

612 22.Weiner, L. M.; Surana, R.; Wang, S., Monoclonal antibodies: versatile platforms for cancer
613 immunotherapy. *Nature Reviews Immunology* **2010**, *10* (5), 317-327.

614 23.Weiner, L. M.; Dhodapkar, M. V.; Ferrone, S., Monoclonal antibodies for cancer immunotherapy. *The*
615 *Lancet* **2009**, *373* (9668), 1033-1040.

616 24.Kingwell, K., CAR T therapies drive into new terrain. *Nature Reviews Drug Discovery* **2017**, *16* (5), 301-
617 304.

618 25.Widakowich, C.; de Castro Jr, G.; de Azambuja, E.; Dinh, P.; Awada, A., Review: Side Effects of
619 Approved Molecular Targeted Therapies in Solid Cancers. *The Oncologist* **2007**, *12* (12), 1443-1455.

620 26.Stern, M.; Herrmann, R., Overview of monoclonal antibodies in cancer therapy: present and promise.
621 *Critical Reviews in Oncology/Hematology* **2005**, *54* (1), 11-29.

622 27.Gharwan, H.; Groninger, H., Kinase inhibitors and monoclonal antibodies in oncology: clinical
623 implications. *Nature Reviews Clinical Oncology* **2016**, *13* (4), 209-227.

624 28.Hansel, T. T.; Kropshofer, H.; Singer, T.; Mitchell, J. A.; George, A. J. T., The safety and side effects of
625 monoclonal antibodies. *Nature Reviews Drug Discovery* **2010**, *9* (4), 325-338.

626 29.Pichler, W.; Campi, P., Adverse Side Effects to Biological Agents. **2007**, 151-165.

627 30.Shaughnessy, A. F., Monoclonal antibodies: magic bullets with a hefty price tag. *BMJ : British Medical*
628 *Journal* **2012**, *345*, e8346.

629 31.Moorkens, E.; Jonker-Exler, C.; Huys, I.; Declerck, P.; Simoens, S.; Vulto, A. G., Overcoming Barriers to
630 the Market Access of Biosimilars in the European Union: The Case of Biosimilar Monoclonal Antibodies.
631 *Frontiers in Pharmacology* **2016**, *7*, 193.

632 32.Deslouches, B.; Peter Di, Y., Antimicrobial peptides with selective antitumor mechanisms: prospect for
633 anticancer applications. *Oncotarget; Vol 8, No 28* **2017**.

634 33.Felício, M. R.; Silva, O. N.; Gonçalves, S.; Santos, N. C.; Franco, O. L., Peptides with Dual Antimicrobial
635 and Anticancer Activities. *Frontiers in Chemistry* **2017**, *5*, 5.

636 34.Gaspar, D.; Veiga, A. S.; Castanho, M. A. R. B., From antimicrobial to anticancer peptides. A review.
637 *Frontiers in Microbiology* **2013**, *4*, 294.

638 35.Riedl, S.; Zweytick, D.; Lohner, K., Membrane-active host defense peptides – Challenges and
639 perspectives for the development of novel anticancer drugs. *Chemistry and Physics of Lipids* **2011**, *164* (8),
640 766-781.

641 36.Hoskin, D. W.; Ramamoorthy, A., Studies on anticancer activities of antimicrobial peptides. *Biochimica et*
642 *Biophysica Acta (BBA) - Biomembranes* **2008**, *1778* (2), 357-375.

643 37.Nyström, L.; Malmsten, M., Membrane interactions and cell selectivity of amphiphilic anticancer
644 peptides. *Current Opinion in Colloid & Interface Science* **2018**, *38*, 1-17.

645 38.Wu, D.; Gao, Y.; Qi, Y.; Chen, L.; Ma, Y.; Li, Y., Peptide-based cancer therapy: Opportunity and
646 challenge. *Cancer Letters* **2014**, *351* (1), 13-22.

647 39.Schweizer, F., Cationic amphiphilic peptides with cancer-selective toxicity. *European Journal of*
648 *Pharmacology* **2009**, *625* (1), 190-194.

649 40.Gong, H.; Zhang, J.; Hu, X.; Li, Z.; Fa, K.; Liu, H.; Waigh, T. A.; McBain, A.; Lu, J. R., Hydrophobic
650 Control of the Bioactivity and Cytotoxicity of de Novo-Designed Antimicrobial Peptides. *ACS Applied*
651 *Materials & Interfaces* **2019**, *11* (38), 34609-34620.

652 41.Chen, C.; Yang, C.; Chen, Y.; Wang, F.; Mu, Q.; Zhang, J.; Li, Z.; Pan, F.; Xu, H.; Lu, J. R., Surface
653 Physical Activity and Hydrophobicity of Designed Helical Peptide Amphiphiles Control Their Bioactivity and
654 Cell Selectivity. *ACS Applied Materials & Interfaces* **2016**, *8* (40), 26501-26510.

655 42.Yeung, A. T. Y.; Gellatly, S. L.; Hancock, R. E. W., Multifunctional cationic host defence peptides and their
656 clinical applications. *Cellular and Molecular Life Sciences* **2011**, *68* (13), 2161.

657 43.Ong, Z. Y.; Wiradharma, N.; Yang, Y. Y., Strategies employed in the design and optimization of synthetic
658 antimicrobial peptide amphiphiles with enhanced therapeutic potentials. *Advanced Drug Delivery Reviews*
659 **2014**, *78*, 28-45.

660 44.Grisoni, F.; Neuhaus, C. S.; Hishinuma, M.; Gabernet, G.; Hiss, J. A.; Kotera, M.; Schneider, G., De novo
661 design of anticancer peptides by ensemble artificial neural networks. *Journal of Molecular Modeling* **2019**,
662 *25* (5), 112.

663 45.Lin, Y.-C.; Lim, Y. F.; Russo, E.; Schneider, P.; Bolliger, L.; Edenharter, A.; Altmann, K.-H.; Halin, C.;
664 Hiss, J. A.; Schneider, G., Multidimensional Design of Anticancer Peptides. *Angewandte Chemie*
665 *International Edition* **2015**, *54* (35), 10370-10374.

666 46.Tyagi, A.; Kapoor, P.; Kumar, R.; Chaudhary, K.; Gautam, A.; Raghava, G. P. S., In Silico Models for
667 Designing and Discovering Novel Anticancer Peptides. *Scientific Reports* **2013**, *3* (1), 2984.

668 47.Gabernet, G.; Gautschi, D.; Müller, A. T.; Neuhaus, C. S.; Armbrrecht, L.; Dittrich, P. S.; Hiss, J. A.;
669 Schneider, G., In silico design and optimization of selective membranolytic anticancer peptides. *Scientific*
670 *Reports* **2019**, *9* (1), 11282.

671 48.Zelezetsky, I.; Tossi, A., Alpha-helical antimicrobial peptides—Using a sequence template to guide
672 structure–activity relationship studies. *Biochimica et Biophysica Acta (BBA) - Biomembranes* **2006**, *1758* (9),
673 1436-1449.

674 49.Ong, Z. Y.; Gao, S. J.; Yang, Y. Y., Short Synthetic β -Sheet Forming Peptide Amphiphiles as Broad
675 Spectrum Antimicrobials with Antibiofilm and Endotoxin Neutralizing Capabilities. *Advanced Functional*
676 *Materials* **2013**, *23* (29), 3682-3692.

677 50.Ong, Z. Y.; Cheng, J.; Huang, Y.; Xu, K.; Ji, Z.; Fan, W.; Yang, Y. Y., Effect of stereochemistry, chain
678 length and sequence pattern on antimicrobial properties of short synthetic β -sheet forming peptide
679 amphiphiles. *Biomaterials* **2014**, *35* (4), 1315-1325.

680 51.Wu, H.; Ong, Z. Y.; Liu, S.; Li, Y.; Wiradharma, N.; Yang, Y. Y.; Ying, J. Y., Synthetic β -sheet forming
681 peptide amphiphiles for treatment of fungal keratitis. *Biomaterials* **2015**, *43*, 44-49.

682 52.Chen, C.; Hu, J.; Zhang, S.; Zhou, P.; Zhao, X.; Xu, H.; Zhao, X.; Yaseen, M.; Lu, J. R., Molecular
683 mechanisms of antibacterial and antitumor actions of designed surfactant-like peptides. *Biomaterials* **2012**,
684 *33* (2), 592-603.

685 53.Travkova, O. G.; Moehwald, H.; Brezesinski, G., The interaction of antimicrobial peptides with
686 membranes. *Advances in Colloid and Interface Science* **2017**, *247*, 521-532.

687 54.Boohaker, R. J.; Zhang, G.; Lee, M. W.; Nemeč, K. N.; Santra, S.; Perez, J. M.; Khaled, A. R., Rational
688 Development of a Cytotoxic Peptide To Trigger Cell Death. *Molecular Pharmaceutics* **2012**, *9* (7), 2080-2093.

689 55.Wimley, W. C., Toward genomic identification of β -barrel membrane proteins: Composition and
690 architecture of known structures. *Protein Science* **2002**, *11* (2), 301-312.

691 56.Smith, C. K.; Withka, J. M.; Regan, L., A Thermodynamic Scale for the β -Sheet Forming Tendencies
692 of the Amino Acids. *Biochemistry* **1994**, *33* (18), 5510-5517.

693 57.Minor, D. L.; Kim, P. S., Measurement of the β -sheet-forming propensities of amino acids. *Nature* **1994**,
694 *367* (6464), 660-663.

695 58.Kim, C. A.; Berg, J. M., Thermodynamic β -sheet propensities measured using a zinc-finger host peptide.
696 *Nature* **1993**, *362* (6417), 267-270.

697 59.Mayo, K. H.; Ilyina, E.; Park, H., A recipe for designing water-soluble, β -sheet-forming peptides. *Protein*
698 *Science* **1996**, *5* (7), 1301-1315.

699 60.Dennison, S. R.; Harris, F.; Bhatt, T.; Singh, J.; Phoenix, D. A., The effect of C-terminal amidation on the
700 efficacy and selectivity of antimicrobial and anticancer peptides. *Molecular and Cellular Biochemistry* **2009**,
701 *332* (1), 43.

702 61.Chen, C.; Hu, J.; Zeng, P.; Pan, F.; Yaseen, M.; Xu, H.; Lu, J. R., Molecular mechanisms of anticancer
703 action and cell selectivity of short α -helical peptides. *Biomaterials* **2014**, *35* (5), 1552-1561.

704 62.Chen, C.; Chen, Y.; Yang, C.; Zeng, P.; Xu, H.; Pan, F.; Lu, J. R., High Selective Performance of Designed
705 Antibacterial and Anticancer Peptide Amphiphiles. *ACS Applied Materials & Interfaces* **2015**, *7* (31), 17346-
706 17355.

707 63.Eisenberg, D.; Weiss, R. M.; Terwilliger, T. C., The helical hydrophobic moment: a measure of the
708 amphiphilicity of a helix. *Nature* **1982**, 299 (5881), 371-374.

709 64.Eisenberg, D.; Schwarz, E.; Komaromy, M.; Wall, R., Analysis of membrane and surface protein
710 sequences with the hydrophobic moment plot. *Journal of Molecular Biology* **1984**, 179 (1), 125-142.

711 65.Pliška, V.; Schmidt, M.; Fauchère, J.-L., Partition coefficients of amino acids and hydrophobic
712 parameters π of their side-chains as measured by thin-layer chromatography. *Journal of Chromatography A*
713 **1981**, 216, 79-92.

714 66.Fauchère, J.-L.; Pliska, V., Hydrophobic parameters Π of amino-acid side chains from the partitioning of
715 N-acetyl-amino-acid amides. *European Journal of Medicinal Chemistry* **1983**, 18 (4), 7.

716 67.Wiradharma, N.; Khoe, U.; Hauser, C. A. E.; Seow, S. V.; Zhang, S.; Yang, Y.-Y., Synthetic cationic
717 amphiphilic α -helical peptides as antimicrobial agents. *Biomaterials* **2011**, 32 (8), 2204-2212.

718 68.Khara, J. S.; Lim, F. K.; Wang, Y.; Ke, X.-Y.; Voo, Z. X.; Yang, Y. Y.; Lakshminarayanan, R.; Ee, P. L. R.,
719 Designing α -helical peptides with enhanced synergism and selectivity against *Mycobacterium smegmatis*:
720 Discerning the role of hydrophobicity and helicity. *Acta Biomaterialia* **2015**, 28, 99-108.

721 69.Hollmann, A.; Martínez, M.; Noguera, M. E.; Augusto, M. T.; Disalvo, A.; Santos, N. C.; Semorile, L.;
722 Maffía, P. C., Role of amphipathicity and hydrophobicity in the balance between hemolysis and peptide–
723 membrane interactions of three related antimicrobial peptides. *Colloids and Surfaces B: Biointerfaces* **2016**,
724 141, 528-536.

725 70.Maget-Dana, R., The monolayer technique: a potent tool for studying the interfacial properties of
726 antimicrobial and membrane-lytic peptides and their interactions with lipid membranes. *Biochimica et*
727 *Biophysica Acta (BBA) - Biomembranes* **1999**, 1462 (1), 109-140.

728 71.Ciumac, D.; Campbell, R. A.; Clifton, L. A.; Xu, H.; Fragneto, G.; Lu, J. R., Influence of Acyl Chain
729 Saturation on the Membrane-Binding Activity of a Short Antimicrobial Peptide. *ACS Omega* **2017**, 2 (11),
730 7482-7492.

731 72.Kim, S.; Kim, S. S.; Lee, B. J., Correlation between the activities of α -helical antimicrobial peptides and
732 hydrophobicities represented as RP HPLC retention times. *Peptides* **2005**, 26 (11), 2050-2056.

733 73.Blondelle, S. E.; Ostresh, J. M.; Houghten, R. A.; Pérez-Payá, E., Induced conformational states of
734 amphipathic peptides in aqueous/lipid environments. *Biophysical Journal* **1995**, 68 (1), 351-359.

735 74.Eiríksdóttir, E.; Konate, K.; Langel, Ü.; Divita, G.; Deshayes, S., Secondary structure of cell-penetrating
736 peptides controls membrane interaction and insertion. *Biochimica et Biophysica Acta (BBA) -*
737 *Biomembranes* **2010**, 1798 (6), 1119-1128.

738 75.Wimley, W. C.; Creamer, T. P.; White, S. H., Solvation Energies of Amino Acid Side Chains and Backbone
739 in a Family of Host–Guest Pentapeptides. *Biochemistry* **1996**, 35 (16), 5109-5124.

740 76.Samanta, U.; Bahadur, R. P.; Chakrabarti, P., Quantifying the accessible surface area of protein residues
741 in their local environment. *Protein Engineering, Design and Selection* **2002**, 15 (8), 659-667.

742 77.Dwyer, D. S., Electronic Properties of the Amino Acid Side Chains Contribute to the Structural
743 Preferences in Protein Folding. *Journal of Biomolecular Structure and Dynamics* **2001**, 18 (6), 881-892.

744 78.Dwyer, D. S., Electronic properties of amino acid side chains: quantum mechanics calculation of
745 substituent effects. *BMC Chemical Biology* **2005**, 5 (1), 2.

746 79.Baud, F.; Karlin, S., Measures of residue density in protein structures. *Proceedings of the National*
747 *Academy of Sciences* **1999**, 96 (22), 12494.

748 80.Zhu, C.; Gao, Y.; Li, H.; Meng, S.; Li, L.; Francisco, J. S.; Zeng, X. C., Characterizing hydrophobicity of
749 amino acid side chains in a protein environment via measuring contact angle of a water nanodroplet on
750 planar peptide network. *Proceedings of the National Academy of Sciences* **2016**, 113 (46), 12946.

751 81.Maget-Dana, R.; Brack, A.; Lelievre, D., Amphiphilic peptides as models for protein-membrane
752 interactions: interfacial behaviour of sequential Lys- and Leu-based peptides and their penetration into lipid
753 monolayers. *Supramolecular Science* **1997**, 4 (3), 365-368.

754 82.Ciumac, D.; Campbell, R. A.; Xu, H.; Clifton, L. A.; Hughes, A. V.; Webster, J. R. P.; Lu, J. R., Implications
755 of lipid monolayer charge characteristics on their selective interactions with a short antimicrobial peptide.
756 *Colloids and Surfaces B: Biointerfaces* **2017**, 150, 308-316.

757 83.Deshayes, S.; Konate, K.; Rydström, A.; Crombez, L.; Godefroy, C.; Milhiet, P.-E.; Thomas, A.;
758 Bresseur, R.; Aldrian, G.; Heitz, F.; Muñoz-Morris, M. A.; Devoisselle, J.-M.; Divita, G., Self-Assembling
759 Peptide-Based Nanoparticles for siRNA Delivery in Primary Cell Lines. *Small* **2012**, 8 (14), 2184-2188.

760 84.Hädicke, A.; Blume, A., Binding of the Cationic Peptide (KL)4K to Lipid Monolayers at the Air–Water
761 Interface: Effect of Lipid Headgroup Charge, Acyl Chain Length, and Acyl Chain Saturation. *The Journal of*
762 *Physical Chemistry B* **2016**, *120* (16), 3880-3887.

763 85.Smiley, S. T.; Reers, M.; Mottola-Hartshorn, C.; Lin, M.; Chen, A.; Smith, T. W.; Steele, G. D.; Chen, L.
764 B., Intracellular heterogeneity in mitochondrial membrane potentials revealed by a J-aggregate-forming
765 lipophilic cation JC-1. *Proceedings of the National Academy of Sciences* **1991**, *88* (9), 3671.

766 86.Reers, M.; Smith, T. W.; Chen, L. B., J-aggregate formation of a carbocyanine as a quantitative
767 fluorescent indicator of membrane potential. *Biochemistry* **1991**, *30* (18), 4480-4486.

768 87.Mancini, M.; Anderson, B. O.; Caldwell, E.; Sedghinasab, M.; Paty, P. B.; Hockenbery, D. M.,
769 Mitochondrial Proliferation and Paradoxical Membrane Depolarization during Terminal Differentiation and
770 Apoptosis in a Human Colon Carcinoma Cell Line. *Journal of Cell Biology* **1997**, *138* (2), 449-469.

771 88.Kulkarni, G. V.; Lee, W.; Seth, A.; McCulloch, C. A. G., Role of Mitochondrial Membrane Potential in
772 Concanavalin A-Induced Apoptosis in Human Fibroblasts. *Experimental Cell Research* **1998**, *245* (1), 170-
773 178.

774 89.Chen, Y.; Guarnieri, M. T.; Vasil, A. I.; Vasil, M. L.; Mant, C. T.; Hodges, R. S., Role of peptide
775 hydrophobicity in the mechanism of action of alpha-helical antimicrobial peptides. *Antimicrobial agents*
776 *and chemotherapy* **2007**, *51* (4), 1398-1406.

777